

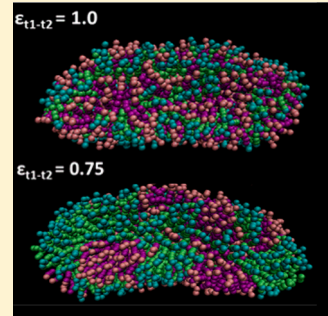
Bioinspired Vesicles Encompassing Two-Tail Phospholipids: Self-Assembly and Phase Segregation via Implicit Solvent Coarse-Grained Molecular Dynamics

Fikret Aydin and Meenakshi Dutt*

Department of Chemical and Biochemical Engineering, Rutgers The State University of New Jersey, Piscataway, New Jersey 08854, United States

Supporting Information

ABSTRACT: Via implicit solvent molecular dynamics simulations, we demonstrate the self-assembly of stable single and binary vesicles composed of two-tail phospholipid molecules. The amphiphilic lipid molecules are composed of a hydrophilic headgroup and two hydrophobic tails and are represented by a reduced coarse-grained model which effectively captures the key chemical and geometric attributes of phospholipid molecules. We report our measurements of the bilayer thickness to be consistent with experimental values reported in the literature. We have probed the role of temperature on the physical properties of single component lipid vesicles and found our results to concur with experimental results. Our investigations on the phase segregation in binary vesicles demonstrate that the degree of distinction between the tail groups of the lipid species can be used to tune their phase segregation in the vesicle bilayer. Finally, our measurements of the scaling exponents for macroscopically phase-segregated systems have been found to be in good agreement with theoretical and simulation studies. Our results can be used for the design of responsive biomaterials for applications in drug delivery, sensing, and imaging.



INTRODUCTION

Biological cell membranes are multicomponent soft materials that can simultaneously act as encapsulating selective barriers promoting intra- and extracellular traffic and active interfacial platforms enabling intracellular communication and cell signaling.¹ The functions of cell membranes are primarily determined by their composition.² These bilayer membranes are composed of amphiphilic molecular species composed of hydrophilic groups which are exposed to the exterior of the bilayer and the cytoplasm and hydrocarbon groups which constitute the hydrophobic region of the membrane.^{1,3} Lipid bilayers are formed when the amphiphilic molecular species introduced into a hydrophilic solvent environment self-assemble to shield the hydrophobic entities from the solvent.¹ The hydrophilic and hydrophobic groups of the different molecular species comprise of distinct chemical moieties which endow unique molecular geometry, functionality, and melting temperature. The diversity in the molecular geometry, chemistry, and functionality of the various species enables the cell membrane to dynamically respond to changes in environmental cues and processes in the vicinity of the bilayer–solvent interface. The active nature of the cell membranes allows it to modulate its tension via the reorganization of its molecular constituents, thereby facilitating a multitude of cellular functionalities such as interfacial binding,^{1,3} fusion, budding, and vesiculation events.^{4,5} For example, cells can maintain their mechanical properties under a range of thermal conditions by adjusting the molecular composition of their membrane.^{2,6} Differences in the molecular species in the membranes enable their self-organization into

domains or rafts^{7–21} which have been shown to be critical for the interfacial binding events on the cell surface,^{22,23} responsible for promoting intra- and extracellular communication. A fundamental understanding of the physicochemical mechanisms driving the formation of domains and rafts in membranes will enhance the development of novel therapeutic approaches targeting these processes. We are interested in investigating the role of the chemical distinction in the hydrocarbon tail group of phospholipids, which is a primary component in cell membranes, on the phase segregation in bioinspired vesicles.

Earlier experimental investigations have demonstrated phase segregation in two-component phospholipid membranes^{24,25} and vesicles.²⁶ These investigations were performed using lipid species with dissimilar polar head groups (and identical hydrocarbon tail groups) or identical polar head groups (and hydrocarbon tail groups of different lengths).^{27–30} Macroscopic phase segregation has also been demonstrated in ternary mixtures encompassing a low melting temperature lipid, a high melting temperature lipid, and cholesterol.^{13,14,31,32} For temperatures below the critical miscibility value, the domain boundaries fluctuate with a correlation length which, along with the hydrodynamic radius, will control the phase segregation.^{15,31,32} For temperatures corresponding to a two-phase region, the initial stages of the phase segregation comprise of the formation of small clusters due to the diffusion, collision,

Received: April 5, 2014

Revised: July 2, 2014

Published: July 2, 2014

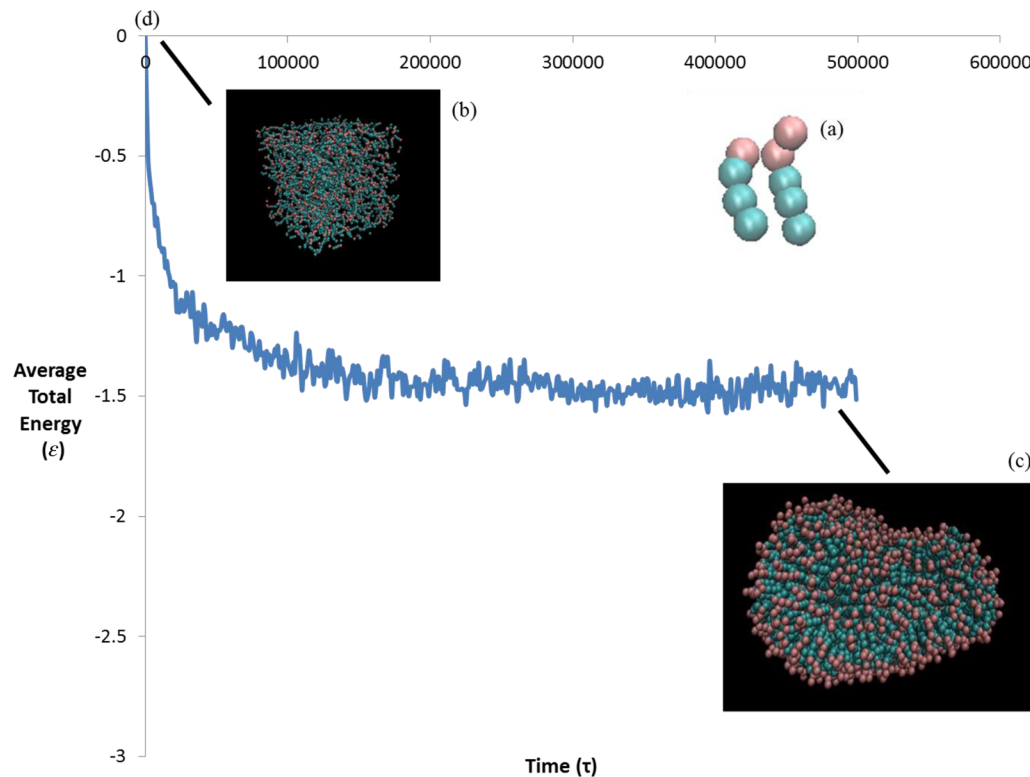


Figure 1. Images of (a) an amphiphilic lipid molecule, (b) randomly dispersed lipid molecules in a simulation box of $25\sigma \times 25\sigma \times 25\sigma$ at the simulation time $t = 0$, (c) a self-assembled single component lipid vesicle at $t = 500000\tau$, and (d) a plot of the average total energy of single component lipid vesicle as a function of time.

and clustering of lipid molecules and is followed by the growth in the sizes of the clusters via the diffusion, collision, and coalescence of the clusters. Experimental^{13,14,31,32} and numerical^{7–12,33–38} studies on coarsening dynamics in multicomponent bilayers have measured the domain growth kinetics and found the kinetics of the latter stage to be determined by the membrane and the surrounding bulk fluid.^{8–10,33,38–40} Earlier studies have identified four key length scales which determine the phase segregation process: the hydrodynamic diameter, the domain size, the correlation length for domains in the vicinity of a critical miscibility limit, and the vesicle diameter.¹³ Numerical studies of coarsening dynamics in multicomponent bilayers must be able to resolve the relevant spatiotemporal scale to capture all stages of the phase segregation process.

All-atom simulations of lipid bilayers that resolve the dynamics of the lipid and water molecules are computationally expensive and limit the investigation to small spatiotemporal scales.^{41–47} These tools are not suitable for addressing phenomena occurring on the mesoscale, such as membrane fusion and rupture, and domain formation in the multicomponent membranes.⁴⁸ Dynamics spanning large length and time scales can be resolved via coarse-graining,^{49–70} implicit solvent approaches,^{41,42,48,50–52,71–74} or mean-field theoretical approaches.^{75–83} Numerical studies have adopted implicit solvent models to investigate phase segregation dynamics via Monte Carlo⁸⁴ and coarse-grained molecular dynamics (MD)⁷ techniques. Other studies have used a MD-based approach entitled dissipative particle dynamics (DPD),^{8–10,33,34,53–60,85–89} which simultaneously resolves both the molecular and continuum scales and reproduces the hydrodynamic behavior, to examine phase segregation in

multicomponent lipid vesicles.^{8–10,33,34,39,40} Continuum approaches^{11,12,38} have also been used to investigate the phase separation dynamics in mixed membranes.

Numerical studies on phase segregation in multicomponent lipid-based systems have used single-tail representation of the constituent molecular species using both MD⁷ and DPD^{8–10,33,39,40} techniques. DPD investigations on two-component vesicles composed of two-tail lipids of different chain length have explored the effect of the relative concentration of one of the lipid species on the mechanical properties of the vesicles.³⁴ We have focused our investigations on the phase segregation in binary vesicles composed of two-tail phospholipid molecular species via an implicit solvent coarse-grained MD approach.

In this paper, we use a reduced model⁴⁸ for a two-tail phospholipid molecule to investigate the formation of one and two species phospholipid vesicles (via self-assembly), and the phase segregation in a binary vesicle, for different degrees of chemical distinction between the hydrocarbon tail groups. The chemical distinction in the hydrocarbon tail groups can arise due to different chemical moieties, chain length, or molecular geometry. This model is based on the use of broad attractive potentials between the hydrocarbon tail beads and enables the formation of fluid lipid bilayer, in the absence of solvent. Our measurements of the scaling exponents for the coarsening dynamics in a binary system which has demonstrated macroscopic phase segregation are in good agreement with theoretical and simulation studies.^{7,90–92} Our results could potentially be used to design novel responsive biocompatible vehicles for targeted delivery of therapeutic, sensing, or imaging agents.^{93–95} We would like to note that another implicit solvent model⁷ has been used to study phase segregation in binary

vesicles composed of single-tail representations of the molecular species.

METHODOLOGY

The particle dynamics can be resolved by using classical molecular dynamics (MD) simulations.^{96–98} The equation of motion for each bead i is given by $\mathbf{F}_i = m_i \mathbf{a}_i$, where \mathbf{F}_i is the force acting on bead i , m_i is the mass, and \mathbf{a}_i is the acceleration of the bead i . The force can be expressed as the gradient of the potential energy U by the relations $\mathbf{F}_i = -\nabla_i U$ with $U = U_{\text{pair}} + U_{\text{bond}} + U_{\text{angle}}$, where U_{pair} , U_{bond} , and U_{angle} are the potential energies from all its pair, bond, and angle interactions, respectively. The dynamics of each bead i can be determined by the following equations: $-\nabla_i U = m_i \mathbf{a}_i = m_i (\partial^2 \mathbf{r}_i / \partial t^2) = m_i (\partial \mathbf{v}_i / \partial t)$ and $\mathbf{v}_i = \dot{\mathbf{r}}_i$, where \mathbf{r}_i and \mathbf{v}_i are the position and velocity vectors of bead i . The equations of motion will be integrated using the velocity Verlet method⁹⁸ which has greater stability and time reversibility and preserves the symplectic form in the phase space compared to the Euler method.⁹⁸ The MD simulations will sample the canonical ensemble and will be run using the open source parallelized MD program called LAMMPS.⁹⁹

In this paper, we use a coarse-grained model of a two-tail phospholipid molecule (see Figure 1a) and demonstrate the formation of a stable vesicle via self-assembly, as shown in Figure 1c. We also investigate the role of the effective distinction between two amphiphilic lipid species on the formation of a stable binary vesicle and their phase segregation in the bilayer. The dissimilarity in the amphiphilic lipid species can arise due to differences in the chemistry of the head or tail groups, the length of the hydrocarbon tails, or the molecular geometry of the lipid molecule and can be modeled effectively through suitable pair potential interaction parameters.

We have adopted a model introduced by Cooke and Deserno⁴⁸ and used it for developing an implicit solvent coarse-grained representation of dipalmitoylphosphatidylcholine (DPPC) phospholipid molecule. Cooke and Deserno⁴⁸ use the model to study bilayers formed from a single tail lipid molecule. The physics of the model is controlled by the external temperature (i.e., $k_B T$) which determines the entropy and the interaction energy (ϵ) which sets the enthalpy. The ratio $k_B T / \epsilon$ determines the phase behavior of the bilayer⁴⁸ and is the same for all the beads, for a given value of the interaction energy. This enables us to adopt the model for a two-tail representation of a phospholipid molecule. A lipid molecule is represented by a bead–spring model with one headgroup encompassing three hydrophilic beads and two hydrocarbon tail groups composed of three hydrophobic beads each, as shown in Figure 1a. The repulsive interactions due to the excluded volume effects between the beads can be modeled by the purely repulsive Weeks–Chandler–Andersen (WCA) soft-sphere potential¹⁰⁰ $U_{\text{rep}}(r, b) = 4\epsilon[(b/r)^{12} - (b/r)^6] + \epsilon$ (for $r \leq r_c$), where ϵ is the depth of the potential well, b is the bead diameter, r is the distance between two beads, and r_c is the cutoff distance beyond which the interactions are not computed. The cutoff distance is chosen as $r_c = 2^{1/6}b$. The interaction between the head–head and the head–tail beads is purely repulsive and is represented by the WCA potential. The hydrophobic effect arising from the van der Waals attraction between the beads can be suitably represented by a Lennard-Jones-style potential with its range extended via a tunable length w_f : $U_{\text{flat}}(r) = -\epsilon$ (for $r < r_c + w_f$), $U_{\text{flat LJ}}(r) = 4\epsilon[(b/(r - w_f))^{12} - (b/(r - w_f))^6]$ (for $r_c \leq r \leq w_f + w_{\text{cut}}$) and $U_{\text{flat LJ}}(r) = 0$ (for $r > w_f + w_{\text{cut}}$), where the potential is cutoff beyond $w_f + w_{\text{cut}}$.⁴⁸ The underlying principle of this model is the use of a broad attractive potential $U_{\text{flat LJ}}(r)$ between the tail beads to compensate for the absence of the solvent molecules. Here, w_f is the length of the flat region at the minimum of potential and w_{cut} is the cutoff distance. In our simulations, we choose $w_f = 0.2\sigma$ and $w_c = 2.5\sigma$. The value of r_c depends on the type of beads interacting with each other, and it is controlled by setting the value of b . For the head–head and head–tail interactions, b is set to be 0.95σ , and for tail–tail interactions, b is set to be σ . ϵ is the unit of energy, and σ is the unit of length. The interaction between the tail beads is obtained by combining the repulsive and attractive pair potentials to yield a combined pair potential U_{comb} of the following form: $U_{\text{comb}}(r) = 4\epsilon[(b/r)^{12} - (b/r)^6]$ (for $r \leq r_c$), $U_{\text{comb}}(r) = -\epsilon$ (for $r_c < r < r_c + w_f$), $U_{\text{comb}}(r) = 4\epsilon[b/(r - w_f)]^{12} - (b/(r - w_f))^6]$ (for $r_c + w_f \leq r \leq w_f + w_{\text{cut}}$), and $U_{\text{comb}}(r) = 0$ (for $r > w_f + w_{\text{cut}}$). The dissimilarity in the amphiphilic lipid species is modeled effectively through the pair potential interaction parameter ϵ . For a system composed of a single species of lipid molecules, the value of ϵ is set to 1. We model mixtures of lipid species with distinct tail groups via the pair potential interaction energy ϵ to capture the interactions between the tail beads of the like and unlike lipid species. We use the depth of the attractive potential represented by ϵ to effectively capture the dissimilarities in the chemistry or the length of the hydrocarbon tails or the molecular geometry of the two lipid species. We would like to note that values of the pair interaction energy ϵ less than 1 implies greater dissimilarity between the two interacting beads.

We draw correspondence between our model and physical systems via the experimental properties of lipid bilayers. We obtain the length scale for our model through the comparison of the experimental measurements of the area per lipid of a DPPC bilayer with similar measurements from our simulations. Experimental measurements of the area per lipid of DPPC bilayers were found to be 64 \AA^2 at 50°C .¹⁰¹ To compute the average area per lipid, the vesicle is divided into 128 small membrane patches such that the average area of each patch is $5.6\sigma^2$. The calculations are performed on particle trajectories output at regular intervals and averaged over all the time steps. The average area per lipid is calculated by taking the arithmetic average of the corresponding values computed for the outer and inner monolayers. Using the value for the area per lipid ($2.39 \sigma^2$) computed for a stable self-assembled single component lipid vesicle, the length scale for our model is $\sigma = 0.52 \text{ nm}$. Using a temperature of 50°C , the energy scale is calculated to be $\epsilon = k_B T = 4.5 \times 10^{-21} \text{ J}$.

In the bead–spring representation of chainlike moieties, two consecutive beads along a chain are connected by an attractive finitely extensible nonlinear elastic spring (FENE)¹⁰⁰ given by $U_{\text{FENE}}(r) = -0.5K r_\infty^{-2} \ln[1 - (r/r_\infty)^2]$ (for $r < r_\infty$) and $U_{\text{FENE}}(r) = \infty$ ($r \geq r_\infty$) where r is the separation of the centers of mass of two bonded beads, r_∞ is the maximum extension of the spring or the divergence length, and K is the spring constant. The stiffness is $K = 30\epsilon/\sigma^2$, and the divergence length is $r_\infty = 1.5\sigma$. The bond potential parameters were selected to model a relatively stiff spring to avoid high-frequency modes and chain crossing.^{48,102} The hydrophobic lipid tails are attributed stiffness through a harmonic angle potential $U_{\text{angle}} = K_\theta(\theta - \theta_0)^2$, where K_θ is the angle potential constant and is given by $8.1 \epsilon/\text{rad}^2$. θ_0 is the equilibrium angle between three consecutively bonded beads and is set to 3.14 rad (or 180°).

Table 1. Tabulation of the Bilayer Thickness and the Area per Lipid of the DPPC Bilayer, at Temperature of $T = 50\text{ }^{\circ}\text{C}^a$

mechanical properties of DPPC bilayer at $50\text{ }^{\circ}\text{C}$	simul results	simul results in physical units	exptl results from the lit.
bilayer thickness	$6.5 \pm 0.1\sigma$	$3.39 \pm 0.06\text{ nm}$	$3.3\text{ nm (theoretical),}^{103} 3.6\text{ nm (AFM)}^{103}$
area per lipid	$2.39 \pm 0.09\sigma^2$	used to obtain length scale	used to obtain length scale

^aMeasurements from the simulations are shown in reduced units (first column) and physical units (second column.) Published experimental and theoretical measurements are provided in the third column. The simulation results in physical units and the experimental results for the area per lipid are not provided since it is used to obtain the length scale of the system and is discussed in the Methodology section.

The simulations were run in the canonical ensemble using the Langevin thermostat with three-dimensional periodic boundary conditions. The simulation box dimensions were set to $25\sigma \times 25\sigma \times 25\sigma$. The total number of beads in the system was 4500, which corresponds to a lipid density of 0.032 lipids per σ^3 . This value corresponds to the lipid density used by Cooke and Deserno.⁴⁸ The simulation time step was set to $\delta t = 0.01\tau$.

The time scale τ was calculated to be 4.9 ns by comparing the experimental measurement of the diffusion coefficient of dipalmitoylphosphatidylcholine (DPPC) bilayer, which is given by $5 \times 10^{-12}\text{ m}^2/\text{s}$,⁵⁹ with that obtained from the simulations. The diffusion coefficient of the lipid molecule in the simulations can be found by tracking the mean-squared displacements of 10 lipid molecules in a vesicle bilayer. We use the relation $\partial\langle r^2(t) \rangle / \partial t = 2dD$ to relate the diffusion coefficient D to the mean-square displacement of a particle in a time interval t .⁹⁶ The variable d is the dimensionality of the system that is given to be 3 for our system. We calculate the diffusion coefficient D to be $0.09\text{ }\sigma^2/\tau$, using the slope of the time evolution of the mean-square displacement. We would like to note that in all our results we have represented time in reduced units.

RESULTS AND DISCUSSION

Self-Assembly of Single Component Lipid Vesicle. For the initial setup, single species of lipid molecules are randomly placed in the simulation box, as shown in Figure 1b. To equilibrate the system, the simulation is run for a time interval of 30000τ with a repulsive pair potential acting between the different types of beads with the temperature set at 1.0. The reduced temperature corresponds to a physical temperature of $50\text{ }^{\circ}\text{C}$ at which the DPPC bilayer is in the fluid state. Following the equilibration phase, the interaction potentials and the corresponding parameters detailed in the Methodology section are used to promote the self-assembly of the amphiphilic lipid molecules to generate a stable single component lipid vesicle, as shown in Figure 1c. Figure 1d shows the time evolution of the average total energy during the self-assembly process. We observe the bond and angle energies to fluctuate about average values for a significant fraction of the aggregation process. The time evolution of the average pair, bond, and angle energies during the self-assembly process have been provided in the Supporting Information (see Figure SI1). We have also investigated the effect of the temperature on the structural characteristics of a single component vesicle. We used a stable self-assembled vesicle as the initial condition and ran simulations for a range of temperatures spanning 0.7 to 0.95. Each simulation was run for an interval of 20000τ . Figure SI2 summarizes the final configurations of the vesicle at the different temperatures and shows the vesicle to remain morphological robust for the values of temperatures explored.

We study the role of temperature on the structure of the vesicles through measurements of the bilayer thickness and the

area per lipid. To calculate the bilayer thickness, the vesicle is divided into multiple small patches so that each patch can be treated effectively as a bilayer membrane. The bilayer thickness is computed by measuring the distance between the lipid head groups in the opposing monolayers in a given patch. These measurements were computed using the particle configuration data obtained from four simulations using identical initial conditions but different random seeds. The bilayer distance was measured for each patch and was averaged over all the patches, the various particle configurations, and the different random seeds. For a single component vesicle, the average bilayer distance is found to be $6.5 \pm 0.1\sigma$, which corresponds to $3.39 \pm 0.06\text{ nm}$ in physical units. We note that this measurement is in fairly good agreement with the theoretical and experimental results for a DPPC bilayer at $50\text{ }^{\circ}\text{C}$, as shown in Table 1.

Details of the average area per lipid measurements are provided in the Methodology section. For a single component vesicle, we find the average area per lipid to be $2.39 \pm 0.09\sigma^2$, as shown in Table 1. Our measurements of the bilayer thickness were not influenced by changes in the temperature, as shown in Table 2. This behavior could manifest from the stiff angle

Table 2. Bilayer Thickness and the Area per Lipid of the Single Component Self-Assembled Vesicle as a Function of Temperature Ranging from 0.7 to 0.95^a

T	bilayer thickness (σ)	area per lipid (σ^2)
0.95	6.5 ± 0.1	2.39 ± 0.09
0.90	6.5 ± 0.1	2.39 ± 0.09
0.85	6.5 ± 0.1	2.4 ± 0.1
0.80	6.5 ± 0.1	2.34 ± 0.09
0.75	6.5 ± 0.1	2.35 ± 0.09
0.70	6.5 ± 0.1	2.33 ± 0.09

^aThe simulations have been run for a total time of 20000τ , and each data point has been averaged over four simulation using different random seeds.

potential functional form that provides greater resistance to variations in the hydrocarbon tail angles, in response to temperature increase. Our computations of the area per lipid, as shown in Table 2, demonstrate a slight increase with the temperature (from $2.33 \pm 0.09\sigma^2$ (or $63 \pm 2\text{ \AA}^2$) at $T = 0.7$ to $2.39 \pm 0.09\sigma^2$ (or $65 \pm 2\text{ \AA}^2$) at $T = 0.95$). This observation is consistent with the theoretical and experimental studies of lipid membranes using X-ray and neutron ULV data.¹⁰⁴ An earlier study¹⁰⁴ has shown increases in the temperature to result in a higher probability of trans-gauche isomerization of the lipid molecules in a bilayer and therefore larger values of the average area per lipid. We do not expect the stiff angle potential functional form to capture the trans-gauche isomerization of the lipid molecules in response to temperature. However, higher temperatures will increase the translational kinetic energy of the molecules in the bilayer plane, resulting in greater spacing between the lipid molecules as demonstrated by

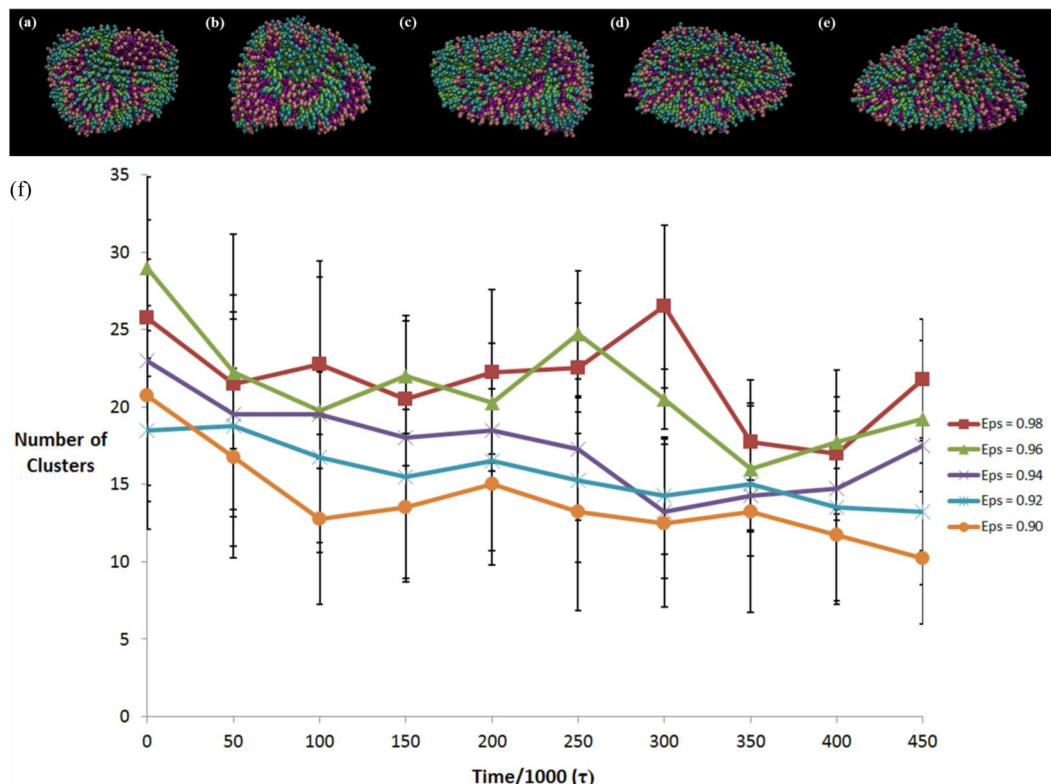


Figure 2. Images of the final configurations of the self-assembled binary vesicle (at time $t = 500000\tau$) for the interspecies intertail bead interaction parameters (a) $\epsilon_{t1-t2} = 0.90$, (b) $\epsilon_{t1-t2} = 0.92$, (c) $\epsilon_{t1-t2} = 0.94$, (d) $\epsilon_{t1-t2} = 0.96$, and (e) $\epsilon_{t1-t2} = 0.98$. (f) Plot of the time evolution of the total number of clusters of one type of lipid species after the formation of a single stable vesicle, for $\epsilon_{t1-t2} = 0.90, 0.92, 0.94, 0.96$, and 0.98 . The simulations have been run for a total time of 500000τ , and each data point has been averaged over four simulation runs using different random seeds. The x-axis has been scaled by $1/1000$ for ease of visualization.

our calculations of the area per lipid. We would like to note that Cook and Deserno measured the area per lipid of their single tail lipid to lie in the range of $1.1\sigma^2$ – $1.5\sigma^2$.⁴⁸

Two Component Lipid Vesicle: Self-Assembly and Phase Segregation. We generate a stable self-assembled vesicle composed of equal concentrations of two species of lipid molecules by using the same protocol to generate a single component vesicle. The two lipid species with chemically distinct tail groups are modeled via the interaction parameter (ϵ_{t1-t2}) between the tail beads of the two lipid types, t_1 and t_2 , which is varied from 0.9 to 0.99. The interaction parameter ϵ between all the other types of beads is set at 1.0. Beginning from a configuration where both types of lipid molecules are dispersed randomly in the simulation box, the spatial and conformational configurations of the lipid molecules are equilibrated by using repulsive interactions between all types of beads. After the equilibration phase, we use parameters that capture the distinct nature of the two lipid species. We observe the lipids to aggregate to form small clusters while the two species phase segregate into small domains, to minimize the energetically less favorable interactions between the dissimilar lipid molecules. After the formation of a single binary vesicle, the clusters composed of like species diffuse in the bilayer, collide, and coalesce to grow in size, thereby reducing the interfacial tension between the different phases in the hydrophobic region of the bilayer. Figure 2a–e summarizes the final configuration of the binary component self-assembled vesicle for different interactions between the tail groups of the two lipid species. Our characterization of the coarsening

dynamics demonstrates the degree of phase separation to increase with the dissimilarity between the tail groups.

We characterize the phase separation in the binary component system by measuring the number of clusters or domains composed of a given type of lipid molecules following the formation of a single vesicle. A cluster is composed of lipids from a given species whose headgroup beads are within interaction range from each other. This definition of a cluster enables us to distinguish between the domains formed in the two monolayers. The lipid molecules in the inner monolayer are more tightly packed as the inner monolayer occupies effectively a spherical shell of smaller volume than the outer monolayer. The difference in the occupied volumes is responsible for an asymmetry in the number of clusters in the two monolayers, as we observe fewer clusters in the inner monolayer.¹⁰⁵

We study the time evolution of the coarsening dynamics by computing the total number of clusters of a given type of lipid molecule following the formation of a stable vesicle, for values of the tail–tail interaction parameter ϵ_{t1-t2} ranging from 0.9 to 0.99. The interfacial tension arising due to the unfavorable energetic interactions between the two lipid species will drive the phase segregation of the lipid species to form multiple domains. We anticipate the interfacial tension to increase with the dissimilarity between the tail groups of the lipid species, thereby inducing the phase segregation process to minimize the interfacial tension by forming fewer clusters of a given lipid type. For sufficiently low interfacial tension, the thermal fluctuations of the mixed bilayer can overcome the energetically favorable interactions between the like lipid species to fragment

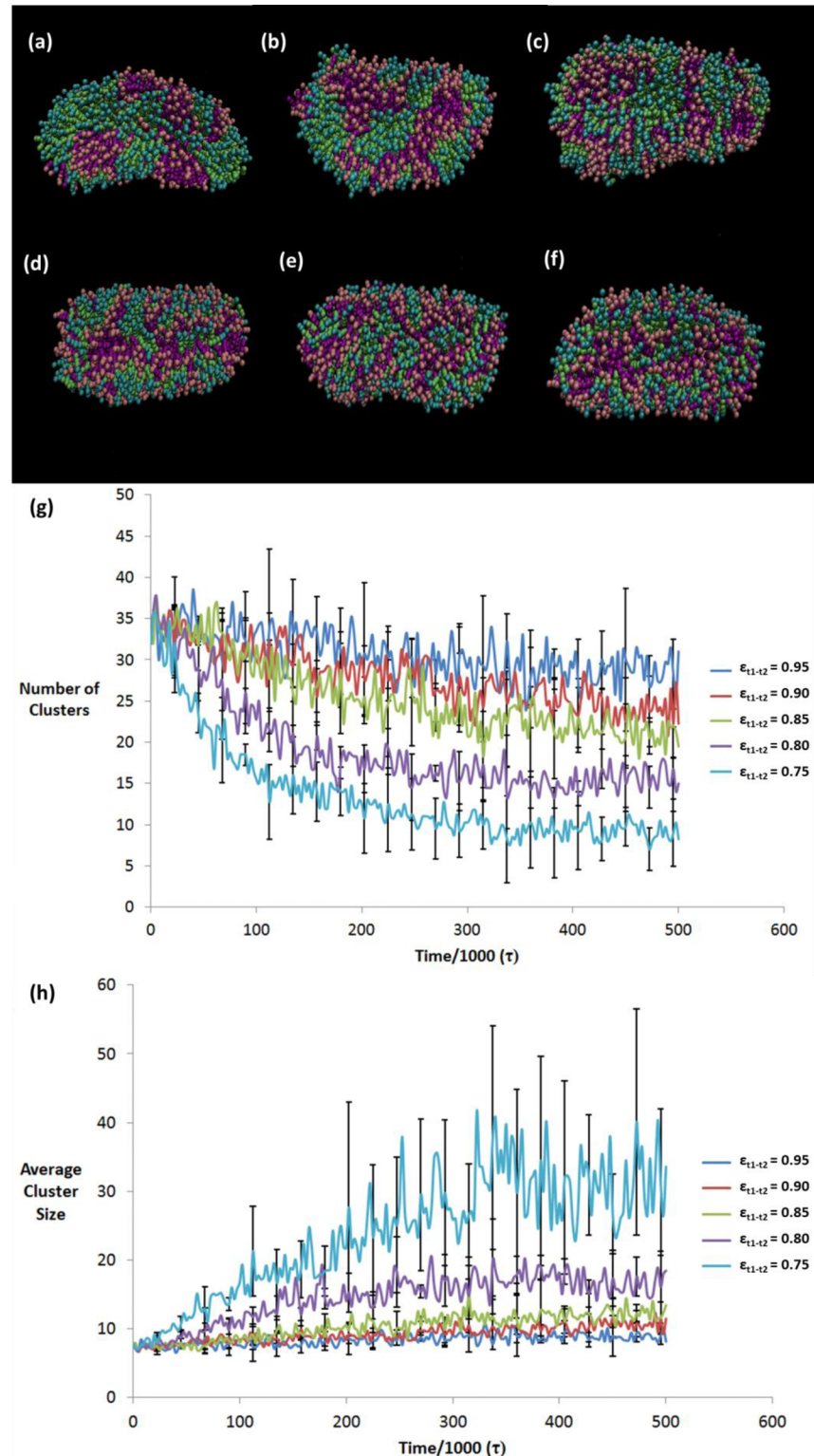


Figure 3. Images of the final configurations of the binary vesicle at $t = 500000\tau$ for the interspecies intertail bead interaction parameters (a) $\epsilon_{t1-t2} = 0.75$, (b) $\epsilon_{t1-t2} = 0.80$, (c) $\epsilon_{t1-t2} = 0.85$, (d) $\epsilon_{t1-t2} = 0.90$, (e) $\epsilon_{t1-t2} = 0.95$, and (f) $\epsilon_{t1-t2} = 1.00$. All the simulations were run beginning from a completely mixed state. Plot of the time evolution of (g) the total number of clusters and (h) the average cluster size, for $\epsilon_{t1-t2} = 0.75, 0.80, 0.85, 0.90$, and 0.95 . The simulations have been run for a total time of 500000τ beginning from a mixed state, and each data point has been averaged over four simulation runs using different random seeds.

the clusters. This process is countered by the minimization of the interfacial energy via the coalescence of clusters composed of a given type of lipids. We observe the cluster growth measurements to support our expectations, as shown in Figure

2f. These computations have used results from four simulations that begin from the same initial conditions but have different random seeds. We would like to note that for temperature-dependent phase segregation in multicomponent bilayers

earlier investigations^{15,31,32} have demonstrated the phase segregation dynamics to be determined by the characteristic correlation length of the fluctuations of the domain boundaries and the hydrodynamic radius, for temperatures below the critical demixing value.

To capture the phase segregation process in the vesicle bilayer beginning from a completely mixed state, we generate a stable self-assembled mixed binary vesicle composed of a 1:1 mixture of two species of lipid molecules by effectively treating both the lipid species as the same species. The binary system can be assumed to behave as a single component system if the interaction energy parameters between the tail beads of the like and unlike lipid species are set to the same value ($\epsilon_{t1-t2} = 1.0$). We follow the same protocol as detailed earlier to generate a self-assembled binary vesicle (shown in Figure 3f) and use the pair potential parameters that capture the distinct nature of each lipid type ($\epsilon_{t1-t2} = 0.75, 0.80, 0.85, 0.90$, and 0.95). Beginning from a mixed configuration, the lipid molecules diffuse in the bilayer, collide, and coalesce to form small domains, to minimize the energetically unfavorable interactions between the dissimilar lipid molecules. The small domains diffuse, collide, and coalesce to grow in size and reduce the interfacial tension between the different phases in the hydrophobic region of the bilayer. We study the phase segregation process by computing the time evolution of the number of clusters composed of a single lipid species and the average cluster size which is defined by the number of molecules in a cluster. These measurements are performed from the time we use the pair potential parameters that are characteristic of the two distinct lipid types. The increasing dissimilarity between the lipid species drives the system to form fewer clusters of larger size. For example, we observe 5–12 clusters in the final configurations of mixtures encompassing highly dissimilar lipids ($\epsilon_{t1-t2} = 0.75$.) Similarly for a lower degree of dissimilarity between the lipid species, as captured by $\epsilon_{t1-t2} = 0.95$, we observe 26–36 clusters in the final configuration. We would like to emphasize that these cluster numbers correspond to the sum of the number of clusters in the inner and outer monolayer of the binary vesicle. We find large error bars are obtained for higher degree of dissimilarity between the tail beads of the two lipid species (see Figure 3h) due to the presence of very few clusters with variation in the cluster sizes.

The time evolution of the coarsening dynamics can be used to compute the scaling exponent of the clustering process by using the relation $N(t) \sim Ct^\alpha$, where $N(t)$ is the number of clusters, C is a constant, t is time, and α is the scaling exponent. Similarly, the growth in the average size of a cluster can be characterized by using the relation $\langle S(t) \rangle \sim Dt^\beta$, where $\langle S(t) \rangle$ is the average size of the clusters, D is a constant, t is time, and β is the scaling exponent. Our measurements of the scaling exponents ($\alpha = 0.50 \pm 0.07$ and $\beta = 0.54 \pm 0.05$) for a system which demonstrates macroscopic phase segregation ($\epsilon_{t1-t2} = 0.75$, see Figure 3a) are in good agreement with theoretical and simulation investigations on phase segregation under non-hydrodynamical conditions.^{7,90–92} We have provided the time evolution of the number of clusters and the average cluster size used to compute the exponents in Figure SI3. The scaling exponents were computed using four simulations with different random seeds which were run for a duration of 1000000τ . We would like to note that for the range of parameters capturing the dissimilarities in the hydrocarbon tail groups we have not observed any budding and vesiculation events.⁹

The composition of the lipid bilayer is expected to influence its thickness and the average area per lipid. We used the same procedure as detailed earlier to measure the bilayer thickness for the binary vesicle, with the interaction parameter ϵ_{t1-t2} between the tail beads of the two lipid species ranging from 0.75 to 0.95. We do not observe any significant differences in the bilayer thickness values for intermediate to low degrees of dissimilarity in the tail groups of the lipid species. Our measurements show a slight decrease in the bilayer thickness (from $6.5 \pm 0.2\sigma$ to $6.4 \pm 0.2\sigma$) for lower values of the tail interaction parameter ϵ_{t1-t2} . We surmise that the slight increase in the bilayer thickness for lower degrees of dissimilarity between the tail groups could be an outcome of the tighter packing of the lipid molecules in the clusters formed in the bilayer. Tighter packing of the lipid molecules could result in less splaying and interdigititation of the lipid tails.

For the binary vesicle, we explore the role of the dissimilarity in the lipid hydrocarbon tail groups on the average area per lipid of the bilayer. We observe the area per lipid to be independent of the different interfacial energies between the distinct lipid species and to be given by $2.4 \pm 0.1\sigma^2$. We surmise that with increasing dissimilarity between the lipid species, the tighter packing of the lipid molecules in the clusters is compensated by low packing density regions adjacent to the periphery of the clusters.

CONCLUSIONS

We have used a model developed by Cooke and Deserno⁴⁸ to simulate single and binary lipid vesicles composed of two-tail amphiphilic lipid molecules. Our characterization results for the bilayer thickness are found to be consistent with the experimental results, as shown in Table 1. Our investigations on the effects of temperature on the physical properties of single component lipid vesicles were found to agree with experimental results. Contrary to expectations, our results demonstrated the bilayer thickness to be independent of temperature. A plausible explanation for this observation could be the use of stiff angle potentials that generates greater resistance to variations in the hydrocarbon tail conformations. Our measurements of the coarsening dynamics in the stable binary component lipid vesicle showed that the degree of phase separation increases with the dissimilarity between the tail groups. We find this observation to be intuitive as the interfacial tension increases with the dissimilarity between the tail groups, driving the phase segregation process to minimize the interfacial tension. Our computation of the scaling exponent for the coarsening dynamics in a system demonstrating macroscopic phase segregation are found to be in good agreement with theoretical and simulations studies.^{7,90–92} Our findings can be used in the design of mesoscopic hybrid nanostructured biomaterials for controlled release applications, such as targeted cancer-drug delivery and bionanotherapeutics.

ASSOCIATED CONTENT

S Supporting Information

Time evolution of the average pair, bond and angle energies during the self-assembly process; the final configurations of the vesicle at the different temperatures; the time evolution of the number of clusters and the average cluster size used to compute the scaling exponents. This material is available free of charge via the Internet at <http://pubs.acs.org>.

AUTHOR INFORMATION

Corresponding Author

*E-mail: meenakshi.dutt@rutgers.edu (M.D.).

Notes

The authors declare no competing financial interest.

ACKNOWLEDGMENTS

All the simulations related to this research were conducted using high performance computational resources at the Rutgers Engineering Computational Cluster.

REFERENCES

- (1) Alberts, B.; Johnson, A.; Lewis, J.; Raff, M.; Roberts, K.; Walter, P. *Molecular Biology of the Cell*; Garland Science: New York, 2007.
- (2) Brannigan, G.; Brown, F. L. H. Composition Dependence of Bilayer Elasticity. *J. Chem. Phys.* **2005**, *122*, 07490.
- (3) Boal, D. *Mechanics of the Cell*; Cambridge University Press: New York, 2012.
- (4) Liang, X.; Mao, G.; Ng, K. Y. S. Mechanical Properties and Stability Measurement of Cholesterol-Containing Liposome on Mica by Atomic Force Microscopy. *J. Colloid Interface Sci.* **2004**, *278*, 53–62.
- (5) Baumgart, T.; Das, S.; Webb, W. W.; Jenkins, J. T. Membrane Elasticity in Giant Vesicles with Fluid Phase Coexistence. *Biophys. J.* **2005**, *89*, 1067–1080.
- (6) Lodish, H.; Baltimore, D.; Berk, A.; Zipursky, S. L.; Matsudaira, P.; Darnell, J. *Molecular Cell Biology*; Scientific American Books: New York, 1995.
- (7) Cooke, I. R.; Kremer, K.; Deserno, M. Tunable Generic Model for Fluid Bilayer Membranes. *Phys. Rev. E* **2005**, *72*, 011506.
- (8) Laradji, M.; Kumar, P. B. S. Dynamics of Domain Growth in Self-assembled Fluid Vesicles. *Phys. Rev. Lett.* **2004**, *93*, 198105.
- (9) Laradji, M.; Kumar, P. B. S. Domain Growth, Budding, and Fission in Phase Separating Self-assembled Fluid Bilayers. *J. Chem. Phys.* **2005**, *123*, 224902.
- (10) Ramachandran, S.; Laradji, M.; Kumar, P. B. S. Lateral Organization of Lipids in Multi-component Liposomes. *J. Phys. Soc. Jpn.* **2009**, *78*, 041006.
- (11) Taniguchi, T. Shape Deformation and Phase Separation Dynamics of Two-Component Vesicles. *Phys. Rev. Lett.* **1996**, *76*, 4444–4447.
- (12) Fan, J.; Han, T.; Haataja, M. Hydrodynamic Effects on Spinodal Decomposition Kinetics in Planar Lipid Bilayer Membranes. *J. Chem. Phys.* **2010**, *133*, 235101.
- (13) Stanich, C. A.; Honerkamp-Smith, A. R.; Putzel, G. G.; Warth, C. S.; Lamprecht, A. K.; Mandal, P.; Mann, E.; Hua, T.-A. D.; Keller, S. L. Coarsening Dynamics of Domains in Lipid Membranes. *Biophys. J.* **2013**, *105*, 444–454.
- (14) Veatch, S. L.; Keller, S. L. Separation of Liquid Phases in Giant Vesicles of Ternary Mixtures of Phospholipids and Cholesterol. *Biophys. J.* **2003**, *85*, 3074–3083.
- (15) Esposito, C.; Tian, A.; Melamed, S.; Johnson, C.; Tee, S.-Y.; Baumgart, T. Flicker Spectroscopy of Thermal Lipid Bilayer Domain Boundary Fluctuations. *Biophys. J.* **2007**, *93*, 3169–3181.
- (16) Lipowsky, R. Budding of Membranes Induced by Intramembrane Domains. *J. Phys. II* **1992**, *2*, 1825.
- (17) Bagatolli, L. A.; Gratton, E. Direct Observation of Lipid Domains in Free Standing Bilayers Using Two-Photon Excitation Fluorescence Microscopy. *J. Fluoresc.* **2001**, *11*, 141–160.
- (18) Ramachandran, S.; Komura, S.; Gommper, G. Effects of an Embedding Bulk Fluid on Phase Separation Dynamics in a Thin Liquid Film. *Europhys. Lett.* **2010**, *89*, S6001.
- (19) Ursell, T. S.; Klug, W. S.; Phillips, R. Morphology and Interaction between Lipid Domains. *Proc. Natl. Acad. Sci. U. S. A.* **2009**, *106*, 13301.
- (20) Bagatolli, L.; Kumar, P. B. S. Phase Behavior of Multicomponent Membranes: Experimental and Computational Techniques. *Soft Matter* **2009**, *5*, 3234–3248.
- (21) Marrink, S. J.; de Vries, A. H.; Tieleman, D. P. Lipids on the Move: Simulations of Membrane Pores, Domains, Stalks and Curves. *Biochim. Biophys. Acta, Biomembr.* **2009**, *1788*, 149–168.
- (22) Lipowsky, R. Domains and Rafts in Membranes—Hidden Dimensions of Selforganization. *J. Biol. Phys.* **2002**, *28*, 195–210.
- (23) Simons, K.; Vaz, W. L. C. Model Systems, Lipid Rafts, and Cell Membranes. *Annu. Rev. Biophys. Biomol. Struct.* **2004**, *3*, 269.
- (24) Wu, S. H. W.; McConnell, H. M. Phase Separations in Phospholipid Membranes. *Biochemistry* **1975**, *14*, 847–854.
- (25) Bagatolli, L. A.; Gratton, E. A Correlation between Lipid Domain Shape and Binary Phospholipid Mixture Composition in Free Standing Bilayers: A Two-Photon Fluorescence Microscopy Study. *Biophys. J.* **2000**, *79*, 434–447.
- (26) Bagatolli, L. A.; Gratton, E. Two Photon Fluorescence Microscopy of Coexisting Lipid Domains in Giant Unilamellar Vesicles of Binary Phospholipid Mixtures. *Biophys. J.* **2000**, *78*, 290–305.
- (27) Leidy, C.; Kaasgaard, T.; Crowe, J. H.; Mouritsen, O. G.; Jorgensen, K. Ripples and the Formation of Anisotropic Lipid Domains: Imaging Two-Component Double Bilayers by Atomic Force Microscopy. *Biophys. J.* **2002**, *83*, 2625–2633.
- (28) Kraft, M. L.; Weber, P. K.; Longo, M. L.; Hutcheon, I. D.; Boxer, S. G. Phase Separation of Lipid Membranes Analyzed with High-Resolution Secondary Ion Mass Spectrometry. *Science* **2006**, *313*, 1948–1951.
- (29) Lin, W. C.; Blanchette, C. D.; Ratto, T. V.; Longo, M. L. Lipid Asymmetry in DLPC/DSPC-Supported Lipid Bilayers: A Combined AFM and Fluorescence Microscopy Study. *Biophys. J.* **2006**, *90*, 228–237.
- (30) Longo, G. S.; Schick, M.; Szleifer, I. Stability and Liquid-Liquid Phase Separation in Mixed Saturated Lipid Bilayers. *Biophys. J.* **2009**, *96*, 3977–3986.
- (31) Honerkamp-Smith, A. R.; Cicuta, P.; Collins, M. D.; Veatch, S. L.; den Nijs, M.; Schick, M.; Keller, S. L. Line Tensions, Correlation Lengths, and Critical Exponents in Lipid Membranes Near Critical Points. *Biophys. J.* **2008**, *95*, 236–246.
- (32) Honerkamp-Smith, A. R.; Veatch, S. L.; Keller, S. L. An Introduction to Critical Points for Biophysicists; Observations of Compositional Heterogeneity in Lipid Membranes. *Biochim. Biophys. Acta* **2009**, *1788*, 53–63.
- (33) Laradji, M.; Kumar, P. B. S. Anomalously Slow Domain Growth in Fluid Membranes with Asymmetric Transbilayer Lipid Distribution. *Phys. Rev. E: Stat., Nonlinear, Soft Matter Phys.* **2006**, *73*, 040910.
- (34) Illya, G.; Lipowsky, R.; Shillcock, J. C. Two-Component Membrane Material Properties and Domain Formation from Dissipative Particle Dynamics. *J. Chem. Phys.* **2006**, *125*, 114710.
- (35) Kumar, P. B. S.; Gommper, G.; Lipowsky, R. Budding Dynamics of Multicomponent Membranes. *Phys. Rev. Lett.* **2000**, *86*, 3911–3914.
- (36) Imparato, A.; Shillcock, J. C.; Lipowsky, R. Lateral and Transverse Diffusion in Two-component Bilayer Membranes. *Eur. Phys. J. E* **2003**, *11*, 21–28.
- (37) Hu, J.; Weikl, T.; Lipowsky, R. Vesicles with Multiple Membrane Domains. *Soft Matter* **2011**, *7*, 6092.
- (38) Brown, F. L. H. Continuum Simulations of Biomembrane Dynamics and the Importance of Hydrodynamic Effects. *Q. Rev. Biophys.* **2011**, *44*, 391–432.
- (39) Spangler, E. J.; Laradji, M.; Kumar, P. B. S. Anomalous Freezing Behavior of Nanoscale Liposomes. *Soft Matter* **2012**, *8*, 10896–10904.
- (40) Revalee, J. D.; Laradji, M.; Kumar, P. B. S. Implicit-solvent Mesoscale Model based on Soft-core Potentials for Self-assembled Lipid Membranes. *J. Chem. Phys.* **2008**, *128*, 035102.
- (41) Farago, O. “Water-free” Computer Model for Fluid Bilayer Membranes. *J. Chem. Phys.* **2003**, *119*, 596–605.
- (42) Brannigan, G.; Brown, F. L. H. Solvent-free Simulations of Fluid Membrane Bilayers. *J. Chem. Phys.* **2004**, *120*, 1059.
- (43) Shillcock, J. C. Spontaneous Vesicle Self-Assembly: A Mesoscopic View of Membrane Dynamics. *Langmuir* **2012**, *28*, 541–547.

- (44) Tieleman, D. P.; Leontiadou, H.; Mark, A. E.; Marrink, S. J. Simulation of Pore Formation in Lipid Bilayers by Mechanical Stress and Electric Fields. *J. Am. Chem. Soc.* **2003**, *125*, 6382–6383.
- (45) Damodaran, K. V.; Merz, K. M. A Comparison of DMPC- and DLPE-Based Lipid Bilayers. *Biophys. J.* **1994**, *66*, 1076–1087.
- (46) Moore, P. B.; Lopez, C. F.; Klein, M. L. Dynamical Properties of a Hydrated Lipid Bilayer from a Multinanosecond Molecular Dynamics Simulation. *Biophys. J.* **2001**, *81*, 2484–2494.
- (47) Essmann, U.; Perera, L.; Berkowitz, M. L. The Origin of the Hydration Interaction of Lipid Bilayers from MD Simulation of Dipalmitoylphosphatidylcholine Membranes in Gel and Liquid Crystalline Phases. *Langmuir* **1995**, *11*, 4519–4531.
- (48) Cooke, I. R.; Deserno, M. Solvent-free Model for Self-assembling Fluid Bilayer Membranes: Stabilization of the Fluid Phase based on Broad Attractive Tail Potentials. *J. Chem. Phys.* **2005**, *123*, 224710.
- (49) West, B.; Schmid, F. Fluctuations and Elastic Properties of Lipid Membranes in the Gel L-beta State: A Coarse-Grained Monte Carlo Study. *Soft Matter* **2010**, *6*, 1275.
- (50) Farago, O. Mode Excitation Monte Carlo Simulations of Mesoscopically Large Membranes. *J. Chem. Phys.* **2008**, *128*, 184105.
- (51) Farago, O. Fluctuation-induced Attraction between Adhesion Sites of Supported Membranes. *Phys. Rev. E* **2010**, *81*, 050902.
- (52) Farago, O. Membrane Fluctuations near a Plane Rigid Surface. *Phys. Rev. E* **2008**, *78*, 051919.
- (53) Dutt, M.; Nayhouse, M. J.; Kuksenok, O.; Little, S. R.; Balazs, A. C. Interactions of End-Functionalized Nanotubes with Lipid Vesicles: Spontaneous Insertion and Nanotube Self-organization. *Curr. Nanosci.* **2011**, *7*, 699–715.
- (54) Dutt, M.; Kuksenok, O.; Nayhouse, M. J.; Little, S. R.; Balazs, A. C. Modeling the Self-Assembly of Lipids and Nanotubes in Solution: Forming Vesicles and Bicelles with Transmembrane Nanotube Channels. *ACS Nano* **2011**, *5*, 4769–4782.
- (55) Dutt, M.; Kuksenok, O.; Little, S. R.; Balazs, A. C. Forming Transmembrane Channels Using End-Functionalized Nanotubes. *Nanoscale* **2011**, *3*, 240–250.
- (56) Dutt, M.; Kuksenok, O.; Little, S. R.; Balazs, A. C. Designing Tunable Bio-nanostructured Materials via Self-assembly of Amphiphilic Lipids and Functionalized Nanotubes. *MRS Spring 2012 Conf. Proc.* **2012**, 1464.
- (57) Ludford, P.; Aydin, F.; Dutt, M. Design and Characterization of Nanostructured Biomaterials via the Self-assembly of Lipids. *MRS Fall 2013 Conf. Proc.* **2013**, 1498.
- (58) Koufos, E.; Dutt, M. Design of Nanostructured Hybrid Inorganic-biological Materials via Self-assembly. *MRS Spring 2013 Conf. Proc.* **2013**, 1569.
- (59) Smith, K. A.; Jasnow, D.; Balazs, A. C. Designing Synthetic Vesicles that Engulf Nanoscopic Particles. *J. Chem. Phys.* **2007**, *127*, 084703.
- (60) Shillcock, J. C.; Lipowsky, R. Equilibrium Structure and Lateral Stress Distribution of Amphiphilic Bilayers from Dissipative Particle Dynamics Simulations. *J. Chem. Phys.* **2002**, *117*, 5048–5061.
- (61) Goetz, R.; Lipowsky, R. Computer Simulations of Bilayer Membranes: Self-assembly and Interfacial Tension. *J. Chem. Phys.* **1998**, *108*, 7397–7409.
- (62) Kranenburg, M.; Venturoli, M.; Smit, B. Phase Behavior and Induced Interdigitation in Bilayers Studied with Dissipative Particle Dynamics. *J. Phys. Chem. B* **2003**, *107*, 11491.
- (63) Kranenburg, M.; Laforge, C.; Smit, B. Mesoscopic Simulations of Phase Transitions in Lipid Bilayers. *Phys. Chem. Chem. Phys.* **2004**, *6*, 4531–4534.
- (64) Yamamoto, S.; Maruyama, Y.; Hyodo, S. Dissipative Particle Dynamics Study of Spontaneous Vesicle Formation of Amphiphilic Molecules. *J. Chem. Phys.* **2002**, *116*, 5842.
- (65) Yamamoto, S.; Hyodo, S. Budding and Fission Dynamics of Two-Component Vesicles. *J. Chem. Phys.* **2003**, *118*, 7937–7943.
- (66) Stevens, M. J.; Hoh, J. H.; Woolf, T. B. Insights into the Molecular Mechanism of Membrane Fusion from Simulation: Evidence for the Association of Splayed Tails. *Phys. Rev. Lett.* **2003**, *91*, 188102.
- (67) Stevens, M. J. Coarse-Grained Simulations of Lipid Bilayers. *Chem. Phys.* **2004**, *121*, 11942–11948.
- (68) Arkhipov, A.; Yin, Y.; Schulten, K. Membrane-Bending Mechanism of Amphiphysin N-BAR Domains. *Biophys. J.* **2009**, *97*, 2727–2735.
- (69) Shih, A. Y.; Arkhipov, A.; Freddolino, P. L.; Schulten, K. A Coarse-Grained Protein-Lipid Model with Application to Lipoprotein Particles. *J. Phys. Chem. B* **2006**, *110*, 3674–3684.
- (70) Marrink, S. J.; Risselada, H. J.; Yefimov, S.; Tieleman, D. P.; de Vries, A. H. The MARTINI Forcefield: Coarse-Grained Model for Biomolecular Simulations. *J. Phys. Chem. B* **2007**, *111*, 7812–7824.
- (71) Wang, Z.; Frenkel, D. J. Modeling Flexible Amphiphilic Bilayers: A Solvent-free Off-Lattice Monte Carlo Study. *Chem. Phys.* **2005**, *122*, 234711.
- (72) Brannigan, G.; Philips, P. F.; Brown, F. L. H. Flexible Lipid Bilayers in Implicit Solvent. *Phys. Rev. E* **2005**, *72*, 011915.
- (73) Noguchi, H.; Takasu, M. Self-assembly of Amphiphiles into Vesicles: A Brownian Dynamics Simulation. *Phys. Rev. E* **2001**, *64*, 041913.
- (74) Noguchi, H. Fusion and Toroidal Formation of Vesicles by Mechanical Forces: A Brownian Dynamics Simulation. *J. Chem. Phys.* **2002**, *117*, 8130–8137.
- (75) Katsov, K.; Mueller, M.; Schick, M. Field Theoretic Study of Bilayer Membrane Fusion I Hemifusion Mechanism. *Biophys. J.* **2004**, *87*, 3277.
- (76) Schick, M. *Membranes: A Field-Theoretic Description. Encyclopedia of Biophysics*; Roberts, G. C. K., Ed.; Springer-Verlag: Berlin, 2012.
- (77) May, S.; Kozlovsky, Y.; Ben-Shaul, A.; Kozlov, M. M. Tilt Modulus of a Lipid Monolayer. *Eur. Phys. J. E* **2004**, *14*, 299–308.
- (78) May, S. A Molecular Model for the Line Tension of Lipid Membranes. *Eur. Phys. J. E* **2000**, *3*, 37–44.
- (79) Lee, W. B.; Mezzenga, R.; Fredrickson, G. H. Self-Consistent Field Theory for Lipid-based Liquid Crystals: Hydrogen Bonding Effect. *J. Chem. Phys.* **2008**, *128*, 074504–074510.
- (80) Ginzburg, V. V.; Balijepalli, S. Modelling the Thermodynamics of the Interaction of Nanoparticles with Cell Membranes. *Nano Lett.* **2007**, *7*, 3716–3722.
- (81) Ayton, G.; Voth, G. A. Bridging Microscopic and Mesoscopic Simulations of Lipid Bilayers. *Biophys. J.* **2002**, *83*, 3357–3370.
- (82) Wang, Z.-J.; Deserno, M. A Systematically Coarse-Grained Solvent-free Model for Quantitative Phospholipid Bilayer Simulations. *J. Phys. Chem. B* **2010**, *114*, 11207.
- (83) Wang, Z.-J.; Deserno, M. Systematic Implicit Solvent Coarse-Graining of Bilayer Membranes: Lipid and Phase Transferability of the Force Field. *New J. Phys.* **2010**, *12*, 095004.
- (84) Kumar, P. B. S.; Rao, M. Kinetics of Phase Ordering in a Two Component Fluid Membrane. *Mol. Cryst. Liq. Cryst.* **1996**, *288*, 105.
- (85) Groot, R. D.; Warren, P. B. Dissipative Particle Dynamics: Bridging the Gap between Atomistic and Mesoscopic Simulation. *J. Chem. Phys.* **1997**, *107*, 4423–4435.
- (86) Hoogerbrugge, P. J.; Koelman, J. M. V. A. Simulating Microscopic Hydrodynamic Phenomena with Dissipative Particle Dynamics. *Europ. Phys. Lett.* **1992**, *19*, 155.
- (87) Alexeev, A.; Upsal, W. E.; Balazs, A. C. Harnessing Janus Nanoparticles to Create Controllable Pores in Membranes. *ACS Nano* **2008**, *2*, 1117–1122.
- (88) Rekvig, L.; Kranenburg, M.; Vreeide, J.; Hafskjold, B.; Smit, B. Investigation of Surfactant Efficiency Using Dissipative Particle Dynamics. *Langmuir* **2003**, *19*, 8195.
- (89) Gao, L. H.; Shillcock, J. C.; Lipowsky, R. Improved Dissipative Particle Dynamics Simulations of Lipid Bilayers. *J. Chem. Phys.* **2007**, *126*, 015101.
- (90) Gonnella, G.; Orlandini, E.; Yeomans, J. M. Phase Separation in Two-Dimensional Fluids: The Role of Noise. *Phys. Rev. E* **1999**, *59*, 4741.

- (91) Binder, K.; Stauffer, D. Theory for the Slowing Down of the Relaxation and Spinodal Decomposition of Binary Mixtures. *Phys. Rev. Lett.* **1974**, *33*, 1006.
- (92) Ossadnik, P.; Gyure, M. F.; Stanley, H. E.; Glotzer, S. C. Molecular Dynamics Simulation of Spinodal Decomposition in a Two-dimensional Binary Fluid Mixture. *Phys. Rev. Lett.* **1994**, *72*, 2498.
- (93) Langer, R. Perspectives: Drug Delivery – Drugs on Target. *Science* **2001**, *293*, 58–59.
- (94) Venkataraman, S.; Hedrick, J. L.; Ong, Z. Y.; Chuan, Y.; Ee, P. L. R.; Hammond, P. T.; Yang, Y. Y. The Effects of Polymeric Nanostructure Shape on Drug Delivery. *Adv. Drug Delivery Rev.* **2011**, *63*, 1228–1246.
- (95) Eniola, A.; Hammer, D. Artificial Polymeric Cells for Targeted Drug Delivery. *J. Controlled Release* **2003**, *87*, 15–22.
- (96) Frenkel, D.; Smit, B. *Understanding Molecular Simulations: From Algorithms to Applications*; Academic Press: San Diego, 2002.
- (97) Leach, A. R. *Molecular Modeling Principles and Applications*; Addison Wesley Longman: Essex, England, 1996.
- (98) Allen, M. P.; Tildesley, D. J. *Computer Simulations of Liquids*; Clarendon Press: Oxford, 2001.
- (99) <http://lammps.sandia.gov>.
- (100) Chan, E. R.; Ho, L. C.; Glotzer, S. C. Computer Simulations of Block Copolymer Tethered Nanoparticle Self-Assembly. *J. Chem. Phys.* **2006**, *125*, 064905.
- (101) Nagle, J. F.; Tristram-Nagle, S. Structure of Lipid Bilayers. *Biochim. Biophys. Acta* **2000**, *1469*, 159.
- (102) Kremer, K.; Grest, G. S. Dynamics of Entangled Linear Polymer Melts: A Molecular-dynamics Simulation. *J. Chem. Phys.* **1990**, *92*, 5057.
- (103) Leonenko, Z. V.; Finot, E.; Ma, H.; Dahms, T. E. S.; Cramb, D. T. Investigation of Temperature-Induced Phase Transitions in DOPC and DPPC Phospholipid Bilayers Using Temperature-Controlled Scanning Force Microscopy. *Biophys. J.* **2004**, *86*, 3783–3793.
- (104) Kučerka, N.; Nieh, M. P.; Katsaras, J. Fluid Phase Lipid Areas and Bilayer Thicknesses of Commonly Used Phosphatidylcholines as a Function of Temperature. *Biochim. Biophys. Acta* **2011**, *1808*, 2761–2771.
- (105) Campbell, M. K.; Shawn, O. F. *Biochemistry*; Brooks/Cole Cengage Learning: Belmont, CA, 2012.